Mathematics

http://www.aimspress.com/journal/Math

AIMS Mathematics, 9(5): 11423–11431.
DOI: 10.3934/math.2024560
Received: 14 December 2023
Revised: 27 February 2024
Accepted: 11 March 2024
Published: 25 March 2024

Research article

Joint channel training and passive beamforming design for intelligent reflecting surface-aided LoRa systems

Jae-Mo Kang[1] **and Dong-Woo Lim**[2,*]

[1] Department of Artificial Intelligence, Kyungpook National University, Daegu 41566, South Korea
[2] Department of Information & Communication Engineering, Changwon National University, Changwon 51140, South Korea

* **Correspondence:** Email: dwlim@changwon.ac.kr.

Abstract: In order to examine the potential and synergetic aspects of intelligent reflecting surface (IRS) techniques for Internet-of-Things (IoT), we study an IRS-aided Long Range (LoRa) system in this paper. Specifically, to facilitate the acquisition of accurate channel state information (CSI) for effective reflection of LoRa signals, we first propose an optimal training design for the least squares channel estimation with LoRa modulation, and then, by utilizing the acquired CSI, we develop a high-performing passive beamforming scheme based on a signal-to-ratio (SNR) criterion. Numerical results show that the proposed training design considerably outperforms the baseline schemes, and the proposed passive beamforming design results in a significant improvement in performance over that of the conventional LoRa system, thereby demonstrating the feasibility of extending coverage areas of LoRa systems with the aid of IRS.

Keywords: intelligent reflecting surface (IRS); internet-of-things (IoT); long range (LoRa); passive beamforming; channel estimation; training design
Mathematics Subject Classification: 93B51

1. Introduction

Long Range (LoRa) is one of the most widely deployed low-power wide-area network (LPWAN) techniques for Internet-of-Things (IoT) in the world, whose signal modulation is based on a patented chirp spread spectrum [1–13]. Though LoRa is known to strike a good balance between coverage and throughput with low energy consumption, its performance may still be limited in real-world fading environments due to severe path loss [14]. To address this issue and to improve the performance of LoRa over fading channels, a single-input multiple-output (SIMO) LoRa system has been studied in [1]. However, deploying multiple antennas is often costly and practically challenging due to limited hardware cost, size, and complexity.

Recently, an intelligent reflecting surface (IRS), composed of a number of passive and reconfigurable reflective units, has emerged as a cost-, energy-, complexity-efficient alternative to antenna arrays, which effectively reflects incident signals such that a propagation environment becomes better suited for signal reception [15–26]. It also has significant potentials for LoRa in performance improvement; e.g., in [14], the IRS has been used as a means to carry additional information via the differential phase shift keying (DPSK) modulation such that a higher data rate than the conventional LoRa system can be achieved.

The novelty of our work lies that different from [14], in this paper, we consider deploying the IRS to improve the link reliability of the LoRa system. On top of this, the novel contributions of our paper are highlighted as follows:

- For the considered IRS-aided LoRa system, it is imperative to acquire and utilize channel state information (CSI), which is rather a challenging task. Accordingly, we propose the optimal training design for accurate CSI acquisition with LoRa modulation, which has never been reported in the literature.
- Also, considering the errors in the acquired CSI, we derive a closed-form expression of *effective* signal-to-noise ratio (SNR), based on which we optimize the passive beamforming (i.e., reflection pattern) for the IRS.
- Furthermore, various simulation results in realistic propagation environments are presented to validate the superiority and effectiveness of the proposed IRS-aided LoRa system. From the simulation results, useful engineering insights are drawn, which have never been provided in the literature.

2. Signal model

As shown in Figure 1, we consider an IRS-aided LoRa system where an IRS with L reflecting elements is deployed to assist the transmission of LoRa signals from a transmitter (e.g., IoT device or sensor) to a receiver (e.g., gateway or base station), each with a single antenna. [*] In LoRa, the transmitted signal takes the form of an up chirp [1, 28]:

$$x_m(n) = \sqrt{\frac{P}{M}} \exp\left\{ j\frac{\pi(n+m)^2}{M} \right\},\ n = 0, 1, \cdots, M-1 \tag{1}$$

where $P > 0$ is the transmission power and $m \in \{0, 1, \cdots, M-1\}$ denotes a modulation symbol. Let h_0, f_i, and g_i denote complex-valued channel coefficients of the links from the transmitter to the receiver, from the transmitter to the IRS, and from the IRS to the receiver, respectively. The received signal at the receiver is given by

$$y(n) = \left(h_0 + \sum_{i=1}^{L} g_i f_i e^{j\theta_i(n)} \right) x_m(n) + w(n), \quad \forall n \tag{2}$$

[*]Our work for a single antenna can be readily extended to the case with multiple antennas, such that the proposed scheme is applied to each pair of a transmit antenna and a receive antenna.

where $0 \leq \theta_i < 2\pi$ is the phase shift of the ith IRS element, and $w(n)$ is the received noise with zero mean and variance σ^2. Also, $M \triangleq 2^{\mathrm{SF}}$, where $\mathrm{SF} \in \{7, \cdots, 12\}$ denotes the spreading factor. Note that to properly adjust $\{\theta_i(n)\}$ for better signal reflection, one first need to acquire the CSI, i.e., h_0 and $\{f_i g_i\}$, which will be elaborated in the next section.

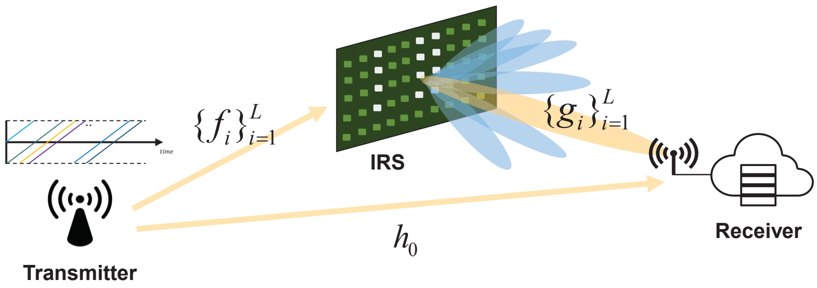

Figure 1. An IRS-aided LoRa system.

3. Optimal training design for LoRa channel estimation

In LoRa, every transmitted frame (or packet) is initiated with a priori known preamble (or training) signal [28], based on which the CSI can be estimated. Typically, the base up chirp (i.e., $\{x_0(n)\}_{n=0}^{M-1}$) is chosen as the preamble signal. The received preamble signal, denoted by $\mathbf{y} \triangleq [y(0), \cdots, y(M-1)]^{\mathsf{T}}$, can be written as

$$\mathbf{y} = \mathbf{X}_\theta \mathbf{h} + \mathbf{w}, \tag{3}$$

where

$$\begin{aligned} &\mathbf{h} \triangleq [h_0, h_1, \cdots, h_L]^{\mathsf{T}}, \quad h_i \triangleq g_i f_i, \quad i = 1, \cdots, L, \\ &\mathbf{X}_\theta \triangleq [\mathbf{x}_0, \mathbf{\Theta}_1 \mathbf{x}_0, \cdots, \mathbf{\Theta}_L \mathbf{x}_0], \; \mathbf{\Theta}_i \triangleq \mathrm{diag}\{e^{j\theta_i(n)}\}_{n=0}^{M-1}, \; \forall i, \\ &\mathbf{x}_0 \triangleq [x_0(0), \cdots, x_0(M-1)]^{\mathsf{T}}, \quad \mathbf{w} \triangleq [w(0), \cdots, w(M-1)]^{\mathsf{T}}. \end{aligned} \tag{4}$$

Assuming that $M \geq L+1$ and $\mathbf{X}_\theta$ is of full-rank, the least squares channel estimate can be obtained as

$$\hat{\mathbf{h}} = \left(\mathbf{X}_\theta^{\mathsf{H}} \mathbf{X}_\theta\right)^{-1} \mathbf{X}_\theta^{\mathsf{H}} \mathbf{y}, \tag{5}$$

for which the estimation mean square error (MSE) is given as $\mathbb{E}[\|\boldsymbol{h} - \hat{\boldsymbol{h}}\|^2] = \sigma^2 \mathrm{tr}[\left(\mathbf{X}_\theta^{\mathsf{H}} \mathbf{X}_\theta\right)^{-1}]$ [29].

The goal of the training design is to minimize the channel estimation MSE by optimizing the reflection pattern of the IRS as

$$(\mathrm{P1}): \quad \underset{0 \leq \theta_i(n) < 2\pi, \forall i, n}{\text{minimize}} \quad \mathrm{tr}\left[\left(\mathbf{X}_\theta^{\mathsf{H}} \mathbf{X}_\theta\right)^{-1}\right].$$

It is known that an optimal solution to the above problem satisfies $\mathbf{X}_\theta^{\mathsf{H}} \mathbf{X}_\theta = \frac{P}{M}\mathbf{I}$ [29]. From (4), this condition is equivalent to[†]

$$\begin{cases} \mathbf{x}_0^{\mathsf{H}}\mathbf{\Theta}_i\mathbf{x}_0 = \sum_{n=0}^{M-1} e^{j\frac{2\pi in}{M}} = 0, & i = 1,\cdots,L \\ \mathbf{x}_0^{\mathsf{H}}\mathbf{\Theta}_i^{\mathsf{H}}\mathbf{\Theta}_\ell\mathbf{x}_0 = \sum_{n=0}^{M-1} e^{j\frac{2\pi(\ell-i)n}{M}} = 0, & 1 \le i \ne \ell \le L \end{cases}, \tag{6}$$

implying that the optimality is achieved when the channel estimation errors become uncorrelated with each other. In general, there exist infinitely many solutions to problem (P1) fulfilling (6). One of the simplest choices is given by the primitive Mth roots of unity as

$$\theta_i(n) = \frac{2\pi in}{M}, \quad i = 1,\cdots,L, \quad n = 0,1,\cdots,M-1. \tag{7}$$

4. Passive beamforming design for LoRa signal reflection

Subsequent to the channel estimation, we now consider the design of the IRS's passive beamforming utilizing the acquired CSI to effectively reflect the incident LoRa signals. Considering the imperfectness of the estimated CSI, the received signal in (2) can be represented as

$$y(n) = \left(\hat{h}_0 + \sum_{i=1}^{L} \hat{h}_i e^{j\theta_i(n)}\right) x_m(n) + \left(\tilde{h}_0 + \sum_{i=1}^{L} \tilde{h}_i e^{j\theta_i(n)}\right) x_m(n) + w(n), \quad \forall n \tag{8}$$

where $\tilde{h}_i \triangleq h_i - \hat{h}_i$, $i = 0,1,\cdots,L$. Note that the first term is the desired signal component, whereas the second term is an additional noise induced by the channel estimation errors. Therefore, from (8), we define the effective SNR as

$$\begin{aligned} \mathrm{SNR}_{\mathrm{eff}} &\triangleq \frac{\mathbb{E}\left[\left|\left(\hat{h}_0 + \sum_{i=1}^{L} \hat{h}_i e^{j\theta_i(n)}\right) x_m(n)\right|^2\right]}{\mathbb{E}\left[\left|\left(\tilde{h}_0 + \sum_{i=1}^{L} \tilde{h}_i e^{j\theta_i(n)}\right) x_m(n) + w(n)\right|^2\right]} \\ &= \frac{P\left|\hat{h}_0 + \sum_{i=1}^{L} \hat{h}_i e^{j\theta_i(n)}\right|^2}{\sigma^2 M(L+2)}. \end{aligned} \tag{9}$$

To enhance the signal detection performance, we aim at maximizing the effective SNR in (9) for each n by optimizing the reflection coefficients of the IRS as follows:

$$\text{(P2)}: \quad \underset{0\le\theta_i<2\pi,\forall i}{\text{maximize}} \quad \left|\hat{h}_0 + \sum_{i=1}^{L} \hat{h}_i e^{j\theta_i}\right|^2, \tag{10}$$

where we drop the index n for simplicity. From the well-known triangle inequality $\left|\hat{h}_0 + \sum_{i=1}^{L} \hat{h}_i e^{j\theta_i}\right| \le \sum_{i=0}^{L} \left|\hat{h}_i\right|$, the solution to problem (P2) can be obtained by achieving the equality as

$$\theta_i = \left(\angle\hat{h}_0 - \angle\hat{h}_i\right)_{\mathrm{mod}\ 2\pi}, \quad i = 1,\cdots,L. \tag{11}$$

It is rather intriguing to note from (11) that the IRS's reflection pattern is fixed when reflecting the LoRa signals, whereas it varies over time when estimating the channels.

[†]To fulfill this optimality condition (i.e., for a proper training), it is required that $M \ge L+1$ (i.e., the number of data measurements for training needs to be larger than that of channel coefficients to be estimated). In LoRa, this requirement is usually met even for a large number of IRS elements (i.e., large value of L) due to a long symbol duration (i.e., large value of M) supported by LoRa. Specifically, LoRa supports six different SF values (from 7 to 12) [5, 28, 33], and thus, the value of M in LoRa ranges from $2^7 = 128$ to $2^{12} = 4096$. In practice, therefore, the value of M (in the order of hundreds or thousands) is usually much larger than that of L (in the order of tens or hundreds).

5. Simulation results

In simulations, we consider an IRS-aided LoRa system with SF = 12. The bandwidth and noise power spectral density are set to 500 kHz[‡] and −174 dBm/Hz,[§] respectively, and thus, the noise variance is $\sigma^2 = -137.01$ dBm. Also, h_0, $\{f_i\}$, and $\{g_i\}$ are modeled as the Rician fading channels with the Rician factor set to 2 and the average path losses given by $d_0^{-\beta}$, $d_f^{-\beta}$, and $d_g^{-\beta}$, respectively, where d_0, d_f, and d_g denote the distances between the transmitter and the receiver, between the transmitter and the IRS, and between the IRS and the receiver, respectively, and β is the path loss exponent. Unless stated otherwise, we use $\beta = 3.2$, $d_f = 2$ m, $d_g = 3$ km,[¶] and $d_0 = \sqrt{d_f^2 + d_g^2}$ throughout the simulations.

In Figure 2, the channel estimation MSE of the proposed training design is shown versus the transmission power P when $L = 16$ (left sub-figure) and versus the number L of reflecting elements at the IRS when $P = -75$ dBm (right sub-figure). In Figure 2, for comparison, we also present the performance of the following baseline schemes:

- *Baseline Scheme I:* A training scheme based on a directional reflection pattern with phase shifts randomly chosen such that $\theta_i(n) \in [-\delta, \delta]$, $\forall i, n$. We set $\delta = 0.035$ rad.
- *Baseline Scheme II:* A training scheme based on an on-off reflection pattern (i.e., $\theta_i(n) \in \{0, 1\}$, $\forall i, n$) such that reflecting elements are sequentially turned on one by one.
- *Baseline Scheme III:* A training scheme based on an alternating optimization of the reflection coefficients $\theta_i(n)$, $\forall i, n$.

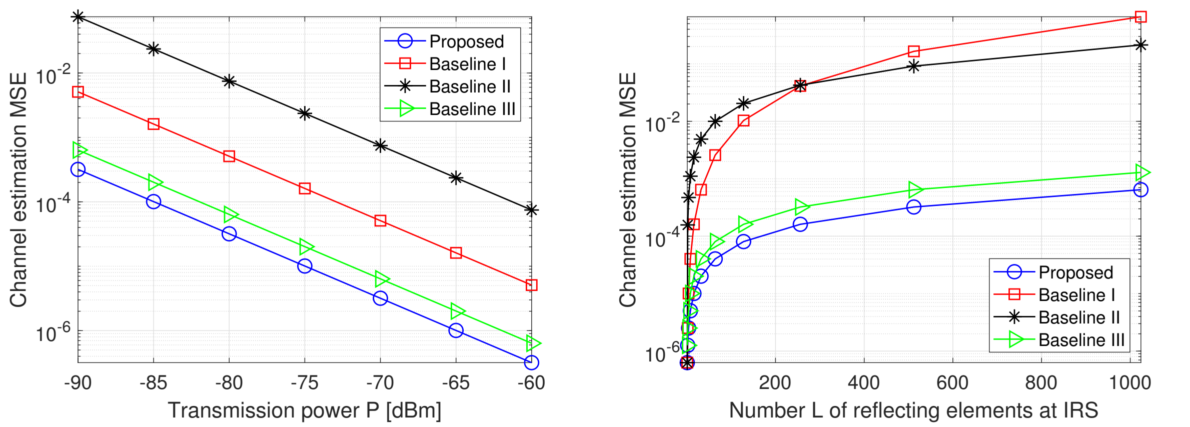

(a) Channel estimation MSE versus P with $L = 16$. (b) Channel estimation MSE versus L with $P = -75$ dBm.

Figure 2. Channel estimation performance of the proposed and baseline schemes.

From Figure 2, it can be seen that the proposed scheme considerably outperforms the baseline schemes. The channel estimation performance of all the schemes improves as P increases (resp. L

[‡]As specified in the standards [5,28,33], LoRa supports three BW settings (125, 250 or 500 kHz) and six different SF values (from 7 to 12).

[§]This corresponds to the thermal noise floor for 1 Hz bandwidth at room temperature (20°C) [34].

[¶]It has been studied in [8] and [30–32] that the coverage of LoRa ranges from 100m to 30km in different scenarios. Therefore, it appears feasible for the LoRa modulation to cover a communication range of 3 km even with the passive IRS.

decreases), because the impact of noise decreases (resp. the number of channel coefficients to be estimated decreases).

In Figure 3, the bit error rate (BER) performance of the following IRS-aided LoRa systems is compared:

- *IRS-aided LoRa I:* The proposed passive beamforming design with CSI estimated by the proposed training design.
- *IRS-aided LoRa II:* The IRS-aided LoRa system with the proposed passive beamforming using perfect CSI.
- *IRS-aided LoRa III:* The IRS-aided LoRa system with an omnidirectional passive beamforming (i.e., $\theta_i = \frac{2\pi i}{L}, \forall i$) using no CSI.
- *Conventional LoRa:* The conventional LoRa system without the IRS.

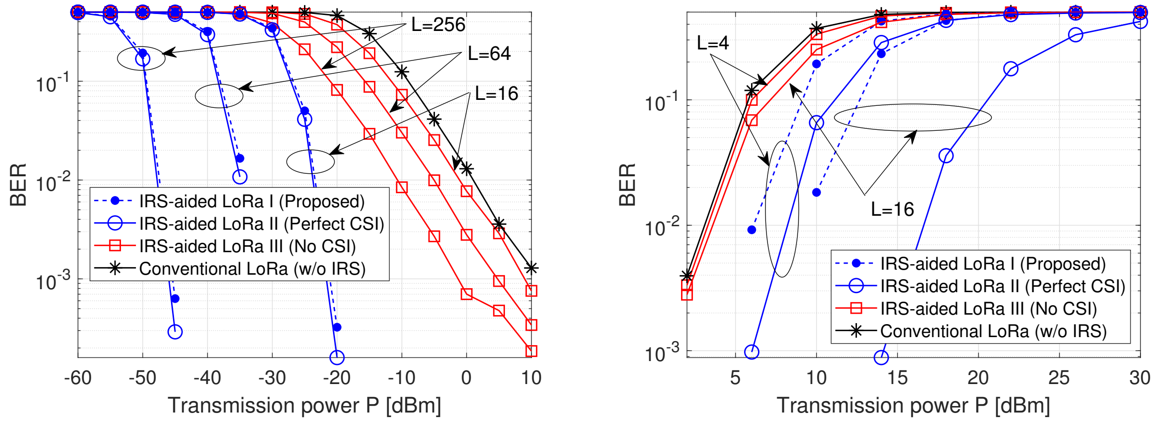

(a) BER versus P with $d_g = 3$ km.

(b) BER versus d_g with $P = 0$ dBm.

Figure 3. BER performance of the various IRS-aided LoRa systems for different L. The CSI is estimated at $P = 0$ dBm.

In the IRS-aided LoRa systems I and II, coherent detection is employed to evaluate the BER performance with estimated CSI and perfect CSI, respectively; whereas, in the IRS-aided LoRa system III and the conventional LoRa system, non-coherent detection is adopted.

In Figure 3, the BERs of the various LoRa systems are shown versus P (left sub-figure) and versus d_g when $P = 0$ dBm (right sub-figure) for different values of L, where for the IRS-aided system I, the CSI is estimated with $P = 0$ dBm. From Figure 3, it can be observed that the IRS-aided LoRa system I yields almost the same performance as the IRS-aided LoRa system II and performs much better than the other systems, thereby validating the effectiveness of the proposed passive beamforming design as well as demonstrating the feasibility of coverage extension of the LoRa system with the aid of IRS. The reason for such superiority is that in the proposed scheme, the channel training and IRS beamforming are jointly optimized such that the IRS beamforming compensates for the CSI errors in the channel training, whereas the other schemes suffer from their suboptimalities. Particularly, the performance improvement of the IRS-aided LoRa system I or II becomes more pronounced as L increases, but that of the IRS-aided LoRa system III is marginal due to the lack of CSI.

6. Conclusions

The optimal training scheme minimizing the channel estimation MSE and the optimal passive beamforming maximizing the effective SNR were derived for the IRS-aided LoRa system, which significantly enhanced the BER performance over the conventional LoRa system.

Use of AI tools declaration

The authors declare they have not used Artificial Intelligence (AI) tools in the creation of this article.

Acknowledgments

This research was supported by the National Research Foundation of Korea(NRF) grant funded by the Korea government(MSIT) (No. 2022R1A4A1033830).

Conflict of interest

All authors declare no conflicts of interest in this paper. The manuscript was written through the contributions of all authors. All authors have approved the final version of the manuscript.

Prof. Jae-Mo Kang is the Guest Editor of special issue "Advances of Artificial Intelligence-based mathematical modeling optimization in engineering applications" for AIMS Mathematics. Prof. Jae-Mo Kang was not involved in the editorial review and the decision to publish this article.

References

1. T. K. Nguyen, H. H. Nguyen, E. Bedeer, Performance improvement of LoRa modulation with signal combining and semi-coherent detection, *IEEE Commun. Lett.*, **25** (2021), 2889–2893. https://doi.org/10.1109/LCOMM.2021.3091997
2. J. M. Kang, MIMO-LoRa for high-data-rate IoT: Concept and precoding design, *IEEE Internet Things J.*, **9** (2022), 10368–10369. https://doi.org/10.1109/JIOT.2022.3143516
3. L. Vangelista, Frequency shift chirp modulation: The LoRa modulation, *IEEE Signal Proc. Lett.*, **24** (2017), 1818–1821. https://doi.org/10.1109/LSP.2017.2762960
4. M. Chiani, A. Elzanaty, On the LoRa modulation for IoT: Waveform properties and spectral analysis, *IEEE Internet Things J.*, **6** (2019), 8463–8470. https://doi.org/10.1109/JIOT.2019.2919151
5. C. Bernier, F. Dehmas, N. Deparis, Low complexity LoRa frame synchronization for ultra-low power software-defined radios, *IEEE T. Commun.*, **68** (2020), 3140–3152. https://doi.org/10.1109/TCOMM.2020.2974464
6. R. Ghanaatian, O. Afisiadis, M. Cotting, A. Burg, LoRa digital receiver analysis and implementation, In: *ICASSP 2019-2019 IEEE International Conference on Acoustics, Speech and Signal Processing (ICASSP)*, 2019. https://doi.org/10.1109/ICASSP.2019.8683504

7. M. Xhonneux, O. Afisiadis, D. Bol, J. Louveaux, A low-complexity LoRa synchronization algorithm robust to sampling time offsets, *IEEE Internet Things J.*, **9** (2022), 3756–3769. https://doi.org/10.1109/JIOT.2021.3101002
8. O. Georgiou, U. Raza, Low power wide area network analysis: Can LoRa scale? *IEEE Wirel. Commun. Lett.*, **6** (2017), 162–165. https://doi.org/10.1109/LWC.2016.2647247
9. O. Afisiadis, S. Li, J. Tapparel, A. Burg, A. Balatsoukas-Stimming, On the advantage of coherent LoRa detection in the presence of interference, *IEEE Internet Things J.*, **8** (2021), 11581–11593. https://doi.org/10.1109/JIOT.2021.3058792
10. T. Elshabrawy, J. Robert, Closed-form approximation of LoRa modulation BER performance, *IEEE Commun. Lett.*, **22** (2018), 1778–1781. https://doi.org/10.1109/LCOMM.2018.2849718
11. O. Afisiadis, M. Cotting, A. Burg, A. Balatsoukas-Stimming, On the error rate of the LoRa modulation with Interference, *IEEE T. Wirel. Commun.*, **19** (2020), 1292–1304. https://doi.org/10.1109/TWC.2019.2952584
12. O. Afisiadis, S. Li, J. Tapparel, A. Burg, A. Balatsoukas-Stimming, On the advantage of coherent LoRa detection in the presence of interference, 2020. arXiv: 2010.00507.
13. D. Croce, M. Gucciardo, S. Mangione, G. Santaromita, I. Tinnirello, Impact of LoRa imperfect orthogonality: Analysis of link-level performance, *IEEE Commun. Lett.*, **22** (2018), 796–799. https://doi.org/10.1109/LCOMM.2018.2797057
14. X. Zhang, W. Xu, G. Cai, Y. Song, G. Chen, A new reconfigurable intelligent-surface-assisted LoRa system, *IEEE T. Veh. Technol.*, **71** (2022), 9055–9060. https://doi.org/10.1109/TVT.2022.3173675
15. Q. Wu, R. Zhang, Towards smart and reconfigurable environment: Intelligent reflecting surface aided wireless network, *IEEE Commun. Mag.*, **58** (2020), 106–112. https://doi.org/10.1109/MCOM.001.1900107
16. S. Gong, X. Lu, D. T. Hoang, D. Niyato, L. Shu, D. I. Kim, et al., Towards smart wireless communications via intelligent reflecting surfaces: A contemporary survey, *IEEE Commun. Surv. Tut.*, **22** (2020), 2283–2314. https://doi.org/10.1109/COMST.2020.3004197
17. J. M. Kang, Intelligent reflecting surface: Joint optimal training sequence and refection pattern, *IEEE Commun. Lett.*, **24** (2020), 1784–1788. https://doi.org/10.1109/LCOMM.2020.2991178
18. B. Zheng, R. Zhang, Intelligent reflecting surface-enhanced OFDM: Channel estimation and reflection optimization, *IEEE Wirel. Commun. Lett.*, **9** (2020), 518–522. https://doi.org/10.1109/LWC.2019.2961357
19. Y. C. Liang, R. Long, Q. Zhang, J. Chen, H. V. Cheng, H. Guo, Large intelligent surface/antennas (LISA): Making reflective radios smart, *J. Commun. Inform. Netw.*, **4** (2019), 40–50. https://doi.org/10.23919/JCIN.2019.8917871
20. Q. Wu, R. Zhang, Intelligent reflecting surface enhanced wireless network: Joint active and passive beamforming design, In: *2018 IEEE Global Communications Conference (GLOBECOM)*, 2018. https://doi.org/10.1109/GLOCOM.2018.8647620
21. Q. Wu, R. Zhang, Intelligent reflecting surface enhanced wireless network via joint active and passive beamforming, *IEEE T. Wirel. Commun.*, **18** (2019), 5394–5409. https://doi.org/10.1109/TWC.2019.2936025

22. X. Yu, D. Xu, R. Schober, MISO wireless communication systems via intelligent reflecting surfaces, In: *2019 IEEE/CIC International Conference on Communications in China (ICCC)*, 2019. https://doi.org/10.1109/ICCChina.2019.8855810
23. H. Guo, Y. C. Liang, J. Chen, E. G. Larsson, Weighted sum-rate maximization for reconfigurable intelligent surface aided wireless networks, *IEEE T. Wirel. Commun.*, **19** (2020), 3064–3076. https://doi.org/10.1109/TWC.2020.2970061
24. M. Zhu, K. Guo, Y. Ye, L. Yang, T. A. Tsiftsis, H. Liu, Active RIS-aided covert communications for MISO-NOMA systems, *IEEE Wirel. Commun. Lett.*, **12** (2023), 2203–2207. https://doi.org/10.1109/LWC.2023.3314625
25. Z. Lu, Y. Zhao, X. Li, C. Z. Xu, Randomized passive energy beamforming for cooperative localization in reconfigurable intelligent surface assisted wireless backscattered sensor network, *IEEE Internet Things J.*, **11** (2023), 9693–9707. https://doi.org/10.1109/JIOT.2023.3323426
26. S. Zhang, R. Zhang, Capacity characterization for intelligent reflecting surface aided MIMO communication, *IEEE J. Sel. Area. Commun.*, **38** (2020), 1823–1838. https://doi.org/10.1109/JSAC.2020.3000814
27. M. Hanif, H. H. Nguyen, Slope-shift keying LoRa-based modulation, *IEEE Internet Things J.*, **8** (2021), 211–221. https://doi.org/10.1109/JIOT.2020.3004318
28. J. Tapparel, *Complete reverse engineering of LoRa PHY*, Available from: `https://www.epfl.ch/labs/tcl/wp-content/uploads/2020/02/Reverse_Eng_Report.pdf`
29. M. Biguesh, A. B. Gershman, Training-based MIMO channel estimation: A study of estimator tradeoffs and optimal training signals, *IEEE T. Signal Proces.*, **54** (2006), 884–893. https://doi.org/10.1109/TSP.2005.863008
30. S. Y. Wang, Y. R. Chen, T. Y. Chen, C. H. Chang, Y. H. Cheng, C. C. Hsu, Performance of LoRa-based IoT applications on campus, In: *2017 IEEE 86th Vehicular Technology Conference (VTC-Fall)*, 2017. https://doi.org/10.1109/VTCFall.2017.8288154
31. K. E. Nolan, W. Guibene, M. Y. Kelly, An evaluation of low power wide area network technologies for the internet of things, In: *2016 International Wireless Communications and Mobile Computing Conference (IWCMC)*, 2016. https://doi.org/10.1109/IWCMC.2016.7577098
32. J. Petajajarvi, K. Mikhaylov, A. Roivainen, T. Hanninen, M. Pettissalo, On the coverage of LPWANs: Range evaluation and channel attenuation model for LoRa technology, In: *2015 14th International Conference on ITS Telecommunications (ITST)*, 2015. https://doi.org/10.1109/ITST.2015.7377400
33. J. Tapparel, O. Afisiadis, P. Mayoraz, A. Balatsoukas-Stimming, A. Burg, An open-source LoRa physical layer prototype on GNU radio, In: *2020 IEEE 21st International Workshop on Signal Processing Advances in Wireless Communications (SPAWC)*, 2020. https://doi.org/10.1109/SPAWC48557.2020.9154273
34. IEEE 802.20 WG, IEEE 802.20 channel models document, IEEE 802.20 PD-08r1, 2007.